



# Quantum regime of a plasma-wave-pumped free-electron laser in the presence of an axial magnetic field

H. Shirvani<sup>a</sup> and S. Jafari<sup>b\*</sup>

<sup>a</sup>Department of Physics, Shahid Beheshti University, GC, Evin, 19834 Tehran, Iran, and <sup>b</sup>Department of Physics, University of Guilan, Rasht 41335-1914, Iran. \*Correspondence e-mail: sjafari@guilan.ac.ir

Received 7 July 2017

Accepted 20 December 2017

Edited by G. Grübel, HASYLAB at DESY, Germany

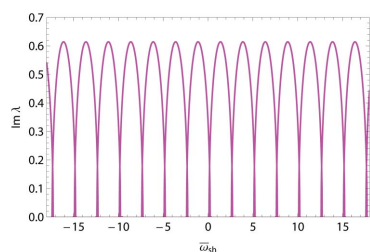
**Keywords:** quantum-FEL; plasma whistler wave; Heisenberg evolution equations; axial magnetic field strength.

The quantum regime of a plasma-whistler-wave-pumped free-electron laser (FEL) in the presence of an axial-guide magnetic field is presented. By quantizing both the plasma whistler field and axial magnetic field, an  $N$ -particle three-dimensional Hamiltonian of quantum-FEL (QFEL) has been derived. Employing Heisenberg evolution equations and introducing a new collective operator which controls the vertical motion of electrons, a quantum dispersion relation of the plasma whistler wiggler has been obtained analytically. Numerical results indicate that, by increasing the intrinsic quantum momentum spread and/or increasing the axial magnetic field strength, the bunching and the radiation fields grow exponentially. In addition, a spiking behavior of the spectrum was observed with increasing cyclotron frequency which provides an enormous improvement in the coherence of QFEL radiation even in a limit close-to-classical regime, where an overlapping of these spikes is observed. Also, an upper limit of the intrinsic quantum momentum spread which depends on the value of the cyclotron frequency was found.

## 1. Introduction

Free-electron lasers (FELs) can produce a radiation pulse with high peak brilliance and with photon energies ranging from the VUV to the X-ray range, *i.e.* from 10 eV (120 nm) to 10 keV (0.12 nm). In general, FEL radiation can be of two different kinds: basic self-emission, which comes from the direct interaction of the electron beam with a wiggler field, and stimulated emission, which occurs when a seed radiation field copropagates with the electron beam. Self-emission occurs starting from random noise in the electron phases. The electrons enter the wiggler in an unprepared state and radiate initial emission. Then the electrons begin to bunch on interacting with the self-radiation and wiggler field, which involves emitting radiation, *i.e.* when the propagation effects become relevant. The FEL self-emission in which the propagation effects are considered is a particular operation mode called self-amplified spontaneous emission (SASE) (Robb & Bonifacio, 2012; Ratner *et al.*, 2015). In the X-ray wavelength range (from a few millimeters to 1 Å or less), a high-gain FEL operated in SASE mode can generate multi-GW and femto-second coherent X-ray pulses.

Considerable efforts have been made to operate FELs at shorter wavelengths and higher powers. In this regard, FEL centers such as FLASH at DESY (Altarelli, 2006; Geloni *et al.*, 2010), LCLS at SLAC (Arthur, 2002), FERMI at Elettra (Allaria *et al.*, 2010) and SCSS in Japan (Tanaka & Shintake, 2005) have focused on producing high-frequency (X-rays) and high-power FELs.



A conventional FEL amplifies coherent radiation by means of a relativistic electron beam passing through a periodic static magnetic field (magnetostatic undulator). The FEL process can be understood as the scattering of virtual undulator photons by the electron beam into photons of the radiation field, *i.e.* an exchange of photons between the undulator and the radiation, with the electrons providing the necessary momentum. This is a resonant process that emits radiation at the resonant wavelength, which indicates that the production of short-wavelength radiation requires either high-energy electron beams or short undulator wavelengths (Schroeder *et al.*, 2001).

There are other alternative strategies for supplying shorter wavelengths (XUV and X-ray) based on two-stage electromagnetically pumped FEL structures, because the Doppler up-shift for such a pump wave is a factor of two higher than a conventional FEL (helical wiggler) with a comparable period (Andriyash *et al.*, 2015; McNeil & Thompson, 2010; Abbasi *et al.*, 2016). In this concept, an electron beam propagates through a helical/planar wiggler located within a resonant cavity; the radiation generated by this device will itself act as an electromagnetic wave wiggler to generate still shorter-wavelength radiation. However, from an experimental point of view, many of these schemes have been difficult to attain, since in many cases the pump wave would act to defocus the electron beam, and also it was difficult to hold the focus of the pump wave over a significant distance to achieve amplification. Another principal difficulty with this concept was that, if the interaction in either stage reaches sufficiently high efficiencies, the electron beam quality could be degraded and could quench both stages of the interaction (Freund & Antonsen, 1996). One of the interesting ways to overcome these problems is to employ plasmas with FELs (Kiselev *et al.*, 2004; Ganeev, 2012). Introducing plasma into the interaction region may confine the electron beam and hold the focus of the pump wave (Sharma & Tripathi, 1996). In addition, the radiation can be confined to some degree by dielectric guiding by the plasma since the dielectric constant in the beam is larger than that of the outside plasma due to the relativistic mass increase of its electron (Ganeev, 2012). The plasma can significantly slow down the radiation mode thereby relaxing the beam energy and beam quality requirements considerably (Jafarinaia *et al.*, 2013). The presence of plasma enables the possibility of employing the plasma modes as wigglers which have a very short period for the excitation of shorter wavelengths (Jafari, 2015). The effective wiggler wavelength in a plasma wiggler is  $\lambda_w = 2\pi c/\omega_p$  or  $\lambda_w$  [cm]  $\simeq 3 \times 10^6/\sqrt{n_p}$  [cm<sup>-3</sup>]. For plasma densities  $n_p$  in the range  $10^{13}$ – $10^{18}$  cm<sup>-3</sup>, the plasma wiggler wavelength  $\lambda_w$  ranges from 1 cm to 30  $\mu$ m (Joshi *et al.*, 1987). Besides, such a FEL, which can produce shorter-wavelength radiation, might provide the opportunity to observe quantum mechanical effects in FEL operation, which in the conventional designs do not play any role (Bonifacio *et al.*, 2005a,b).

The configuration of a quantum-FEL (QFEL) is that of collective Compton backscattering, in which a low-energy electron beam collides with a propagating high-power elec-

tromagnetic wave. The QFEL concept is particularly suited to the generation of very short radiation wavelengths as the photon recoil  $hk$  becomes larger than the spread in electron momentum (Bonifacio *et al.*, 2008). In this regard, operation of a FEL in a quantum regime, in which the spiking behavior observed in the SASE mode disappears and the spectrum reduces to a single narrow line which originates high temporal coherence (quantum purification of SASE) (Bonifacio *et al.*, 2006, 2017; Avetissian & Mkrtchian, 2007), provides an enormous improvement in the coherence of a SASE-FEL X-ray source.

In a FEL, the maximal X-ray photon energy  $2\pi\hbar/\lambda_r$  is limited by the minimal wiggler period and the energy of the electron. In a conventional magnetic wiggler, due to limitations in wiggler wavelength ( $\lambda_w \geq 1$  cm), it is difficult to reach the angstrom radiation wavelengths, which requires large and expensive accelerators. In our work, we tackle this problem by considering a scheme based on a plasma-wave-pumped FEL in the presence of an axial-guide magnetic field. Employing a plasma wiggler provides a very short micrometer undulation period with sufficiently large strength parameter. The purpose of the present paper is to investigate the quantum effects of a plasma-wave wiggler in the presence of an axial-guide magnetic field, in which a relativistic electron beam interacts with a plasma whistler wave. The axial-guide magnetic field is usually present to guide the relativistic electron beam. This work is developed in a linear regime and is conducive to understanding the quantum effects of the cyclotron frequency (caused by the axial-guide magnetic field) on line narrowing. In addition, we demonstrate the higher temporal coherence and more discrete spectrum of the quantum SASE in the presence of an axial-guide magnetic field.

## 2. Physical model

For an experimental realization of a quantum-FEL it is necessary to use an electromagnetic wiggler (such as a laser wiggler or plasma-whistler-wave wiggler) in a collective Compton backscattered configuration, instead of a magnetostatic helical/planer wiggler as employed in classical SASE experiments (Bonifacio *et al.*, 2006, 2007). In a plasma wiggler configuration, a low-energy electron beam backscatters the photons of the whistler wave with a frequency by a factor  $4\gamma^2$ . However, such a choice sets some conditions on the electron beam and wiggler parameters. To avoid two-stream instability due to the beam–plasma interaction, we use an electron beam of length (Joshi *et al.*, 1987)

$$L \leq \frac{c\gamma}{\omega_p} \left( \frac{n_p}{n_{\text{beam}}} \right)^{1/3},$$

where  $n_p$  and  $n_{\text{beam}}$  are the plasma and electron beam densities, respectively. In addition, there is another instability in a plasma-based FEL scheme which is related to the Weibel instability. This instability can be suppressed by beams that are narrower than the plasma skin depth ( $c/\omega_p$ ). As a result, we

employ a short and narrow beam in the plasma-based FEL configuration.

The Hamiltonian of the relativistic electron in the presence of radiation (*i.e.* matter–radiation interaction) in the laboratory frame is

$$H = [m_e^2 c^4 + (\mathbf{P} - e\mathbf{A})^2 c^2]^{1/2}, \quad (1)$$

where  $\mathbf{P} = p_x \hat{e}_x + p_y \hat{e}_y + p_z \hat{e}_z$  is the three-dimensional canonical momentum,  $\mathbf{A}$  is the field vector potential,  $m_e$  and  $e$  are, respectively, the rest mass and charge of the electron, and  $c$  is the speed of light in a vacuum.

In our study the vector potential may be decomposed such that  $\mathbf{A} = \mathbf{A}_r + \mathbf{A}_s + \mathbf{A}_0$ , where  $\mathbf{A}_r$  is the vector potential of the seed radiation field,  $\mathbf{A}_s$  is the vector potential of the whistler wiggler field and  $\mathbf{A}_0$  is the vector potential describing the axial-guide magnetic field which is uniform along the  $z$  axis. Besides, we assume that both the radiation and whistler wiggler wave are propagating in the direction of the  $z$ -axis in the laboratory frame. Therefore these vector potentials in the laboratory frame are

$$\begin{aligned} \mathbf{A}_{r,s} = & A_{r,s}^* \hat{\mathbf{e}} \exp[-i(k_{r,s}z - \omega_{r,s}t)] \\ & + A_{r,s} \hat{\mathbf{e}}^* \exp[i(k_{r,s}z - \omega_{r,s}t)], \end{aligned} \quad (2)$$

$$\mathbf{A}_0 = \left(\sqrt{2}/4\right) B_0 [-(ix + y) \hat{\mathbf{e}} + (ix - y) \hat{\mathbf{e}}^*], \quad (3)$$

where  $(\omega_r, k_r)$  and  $(\omega_s, k_s)$  denote the frequency and wave-number of the radiation and whistler fields, respectively,  $A_{r,s}$  are the amplitude of the vector potentials with  $A_s = A_s^* = -\sqrt{2}B_s/2k_s$  (in which  $B_s$  is the strength of the magnetic field related to the whistler electromagnetic wave), and  $B_0$  is the strength of the axial magnetic field so that  $\mathbf{B} = B_0 \hat{z}$ .  $\hat{\mathbf{e}} = (\hat{e}_x + i\hat{e}_y)/\sqrt{2}$  and  $\hat{\mathbf{e}}^* = (\hat{e}_x - i\hat{e}_y)/\sqrt{2}$  are the unit vector of circular polarization of our fields and it's conjugate, respectively, with vector properties  $\hat{\mathbf{e}} \cdot \hat{\mathbf{e}} = \hat{\mathbf{e}}^* \cdot \hat{\mathbf{e}}^* = 0$  and  $\hat{\mathbf{e}} \cdot \hat{\mathbf{e}}^* = 1$ . This formalism of the vector potentials gives us the convenience to quantize the fields.

The quantum description of a FEL can be in a moving frame, in which we have a non-relativistic problem; however, if one would like a fully relativistic quantum approach there are requirements such as using the Dirac equation (Sen Gupta, 1991; Mandl & Shaw, 2010). However, we will work in a moving frame that moves with the electron beam. The velocity of this frame can be the velocity of the electrons, so that an elastic scattering takes place in which the electron converts a whistler photon into a radiation photon. In a particular moving frame, so-called BR (Bambini & Renieri, 1978), both photons oscillate with the same frequency called the *resonance* frequency (Stenholm & Bambini, 1981).

By using Lorentz transformations from the laboratory frame to the frame moving with normalized velocity  $\beta_f = v_f/c$ , for  $\mathbf{A}_r$  and  $\mathbf{A}_s$  we obtain

$$k_r z - \omega_r t = k' z' - \omega' t', \quad (4)$$

$$k_s z - \omega_s t = -k' z' - \omega' t' \quad (5)$$

and

$$\omega' = \omega_r \gamma_f (1 - \beta_f) = \omega_s \gamma_f (1 + \beta_f), \quad (6)$$

where  $\omega'$  is the resonance frequency,  $\gamma_f = (1 - \beta_f^2)^{-1/2}$  and the prime is used to indicate the moving frame. We assumed the extreme case (San-kui, 1992) where the whistler photon has the same wavenumber as the radiation photon, but opposite to the direction of the moving frame,  $k'_s = -k'_r = -k'$ . In addition, for convenience we will drop the primes hereon with the understanding that all quantities refer to the moving frame. We work in a quantum regime of a FEL starting from noise, so that

$$\frac{e^2 A_r^2}{m_e^2 c^4} \ll \frac{e^2 A_s^2}{m_e^2 c^4} = K^2$$

(Schroeder *et al.*, 2001; Stenholm & Bambini, 1981), where  $K$  is the strength of the whistler wiggler field and is also defined by  $(1 + K^2)^{1/2} = \gamma_\perp$ , in which  $\gamma_\perp$  is the Lorentz factor associated with the transverse motion due to the whistler field.

Now one can quantize the radiation and whistler fields by using the following transformations (Mandl & Shaw, 2010; San-kui, 1992),

$$A_{r,s} \rightarrow \left(\frac{\hbar}{2\varepsilon\omega V}\right)^{1/2} \exp(i\omega t) a_{r,s}, \quad (7)$$

$$A_{r,s}^* \rightarrow \left(\frac{\hbar}{2\varepsilon\omega V}\right)^{1/2} \exp(-i\omega t) a_{r,s}^\dagger, \quad (8)$$

where  $\varepsilon$  is the permittivity of the plasma medium (Freund & Antonsen, 1996; Hedayati *et al.*, 2017),  $V$  is the plasma volume and  $a_{r,s}$  ( $a_{r,s}^\dagger$ ) are the photon annihilation (creation) operators with the commutator  $[a, a^\dagger] = 1$ . In addition, we quantize the axial-guide magnetic field and electron motion through the commutator  $[x_i, p_j] = i\hbar\delta_{ij}$ , where indices imply  $x$ ,  $y$  and  $z$  coordinates.

Then, the three-dimensional Hamiltonian for  $N$  electrons interacting with a single mode radiation and whistler wiggler field in the presence of an axial-guide magnetic field can be found as

$$\begin{aligned} \hat{H} = & mc^2 + \frac{1}{2} \hbar\omega_c + \hbar\omega \\ & + \sum_{j=1}^N \left( \frac{p_{zj}^2}{2m} + mT_j \right. \\ & + \hbar\Omega \left\{ a_s^\dagger a_r \exp[i(\theta_{rs})_j] + a_r^\dagger a_s \exp[-i(\theta_{rs})_j] \right\} \\ & - (m\hbar\Omega)^{1/2} \left\{ a_s^\dagger (T_-)_j \exp[-i(\theta_s)_j] + a_s (T_+)_j \exp[i(\theta_s)_j] \right\} \\ & - (m\hbar\Omega)^{1/2} \left\{ a_r^\dagger (T_-)_j \exp[-i(\theta_r)_j] + a_r (T_+)_j \exp[i(\theta_r)_j] \right\} \left. \right) \\ & + \hbar\omega (a_r^\dagger a_r + a_s^\dagger a_s), \end{aligned} \quad (9)$$

where  $\hat{H}$  is the Hamiltonian operator,  $p_{zj}$  is the  $z$ -component of the momentum operator of the  $j$ th electron,  $\Omega = e^2/2m\varepsilon\omega V$  is the strength of the coupling between the whistler and radiation fields,  $\omega_c = eB_0/m$  is the cyclotron frequency of the electron caused by the axial-guide magnetic field,

and  $(\theta_{rs})_j = (k_r - k_s)z_j = 2kz_j$  is the phase operator of the  $j$ th electron which is entangled between the whistler and radiation fields.

Furthermore,  $(\theta_s)_j = -kz_j$  and  $(\theta_r)_j = kz_j$  are the phase operators of the  $j$ th electron describing its interaction with the whistler and radiation field, respectively,  $m = m_e(1 + K^2)^{1/2} = m_e\gamma_{\perp}$  is the renormalized mass (Schroeder *et al.*, 2001; Stenholm & Bambini, 1981), and

$$(T_+)_j = \frac{[p_{xj} + (eB_0/2)y_j] - i[p_{yj} + (eB_0/2)x_j]}{\sqrt{2m}}, \quad (10)$$

$$(T_-)_j = (T_+)_j^\dagger, \quad (11)$$

$$T_j = (T_+T_-)_j \quad (12)$$

are the the vertical-motion operators (San-kui, 1992) of the  $j$ th electron with commutators

$$\begin{aligned} m[T_+, T_-] &= \hbar\omega_c \\ [mT, T_{\pm}] &= \pm \hbar\omega_c T_{\pm} \end{aligned} \quad (13)$$

and their eigenvalue equations have been described by San-kui (1992). In equation (10),  $P_{xj}$  and  $P_{yj}$  are, respectively, the  $x$ - and  $y$ -components of the momentum operator of the  $j$ th electron.

Physically, the term  $mT + (1/2)\hbar\omega_c$  corresponds to terms  $(\mathbf{A}_0^2)$ ,  $(\mathbf{A}_0 \cdot \mathbf{P})$  and  $(p_x^2 + p_y^2)$ , which control the vertical motion of the electrons with respect to the axial magnetic field.

The transverse operators (10)–(12) are very useful for our purpose in which we will construct a new electron collective operator by using them to take into account the quantum effects of the axial guide in the dispersion relation of the whistler-pumped FEL.

### 3. Heisenberg evolution equations and the dispersion relation

From the Hamiltonian (9) we derive the following Heisenberg evolution equations which determine the dynamics of the QFEL,

$$\frac{d \exp[-i(\theta_{rs})_j]}{dt} = -\frac{i}{2m}(k_r - k_s)[P_z^{(B)}]_j, \quad (14)$$

$$\frac{da_r}{dt} = -i\Omega a_s \sum_{j=1}^N \exp[-i(\theta_{rs})_j] - i\omega a_r + \frac{ib}{\hbar} \sum_{j=1}^N (L_-)_j, \quad (15)$$

$$\frac{d(L_-)_j}{dt} = i\left(\frac{\hbar k^2}{2m} - \omega_c\right)(L_-)_j + \frac{ib}{m}\omega_c a_s \exp[-i(\theta_{rs})_j] + \frac{ib}{m}\omega_c a_r, \quad (16)$$

$$\begin{aligned} \frac{d[P_z^{(B)}]_j}{dt} &= -\frac{i}{2m}\hbar^2(k_r - k_s)^3 \exp[-i(\theta_{rs})_j] \\ &\quad - 2i\hbar\Omega(k_r - k_s)a_s^\dagger a_r \end{aligned} \quad (17)$$

where

$$\begin{aligned} [P_z^{(B)}]_j &= p_{zj} \exp[i(\theta_{rs})_j] + \exp[i(\theta_{rs})_j] p_{zj}, \\ (L_-)_j &= (T_-)_j \exp[-i(\theta_r)_j], \quad b = (m\hbar\Omega)^{1/2}, \end{aligned} \quad (18)$$

and we have used the commutators

$$\begin{aligned} \{\exp[-i(\theta_{rs})_j], p_z\} &= \hbar(k_r - k_s) \exp[-i(\theta_{rs})_j], \\ \{\exp[-i(\theta_r)_j], p_z\} &= \hbar k \exp[-i(\theta_r)_j], \\ [a_l, a_r^\dagger] &= [a_s, a_s^\dagger] = 1, \\ m[T_+, T_-] &= \hbar\omega_c, \\ [mT, T_{\pm}] &= \pm \hbar\omega_c T_{\pm}, \end{aligned}$$

and

$$\begin{aligned} [a_r, a_s^\dagger] &= [a_s, a_r^\dagger] = [a_{r,s}, T_{\pm}] = \{\exp[-i(\theta_{rs})_j], T_{\pm}\} \\ &= [a_{r,s}, p_z] = [p_z, T_{\pm}] = 0. \end{aligned}$$

We work in a linear regime so that the high-order terms in extracting the above equations (14)–(17) are neglected.

From Bonifacio *et al.* (2006), we use the following electron collective operators,

$$B = \frac{1}{\sqrt{N}} \sum_{j=1}^N \exp[-i(\theta_{rs})_j], \quad (19)$$

$$P = \frac{1}{\sqrt{N}} \sum_{j=1}^N \frac{1}{2} [P_z^{(B)}]_j, \quad (20)$$

where,  $[P_z^{(B)}]_j$  is defined in (18),  $B$  denotes the bunching and  $P$  is the symmetrized momentum bunching.

In this manner we introduce a new electron collective operator with respect to the vertical motion of electrons interacting with radiation in the presence of a uniform magnetic field,

$$\mathbf{V}_- = \frac{1}{\sqrt{N}} \sum_{j=1}^N (L_-)_j, \quad (21)$$

where  $(L_-)_j$  is defined in equation (18). By combining equations (19), (20) and (21) with (14)–(17), one can obtain the following relations for the linear regime,

$$\frac{dB}{dt} = -\frac{i}{m}(k_r - k_s)P, \quad (22)$$

$$\frac{da_r}{dt} = -i\sqrt{N}\Omega a_s B - i\omega a_r + \frac{ib}{\hbar}\sqrt{N}\mathbf{V}_-, \quad (23)$$

$$\frac{d\mathbf{V}_-}{dt} = i\left(\frac{\hbar k^2}{2m} - \omega_c\right)\mathbf{V}_- + \frac{ib}{m}\omega_c a_s B + \frac{ib}{m}\sqrt{N}\omega_c a_r, \quad (24)$$

$$\frac{dP}{dt} = -\frac{i}{4m}\hbar^2(k_r - k_s)^3 B - i\sqrt{N}\hbar\Omega(k_r - k_s)a_s^\dagger a_r. \quad (25)$$

We regard the operators  $a_s$  and  $a_s^\dagger$  as follows,

$$a_s, a_s^\dagger \rightarrow \left(\frac{\hbar}{2\varepsilon\omega V}\right)^{-1/2} A_s.$$

Looking for solutions of the linear system (22)–(25) of the form  $B(t) = B_0 \exp(i\lambda t)$ , one can obtain the following normalized characteristic equation as a dispersion relation,

$$[(\bar{\lambda} - \frac{1}{4}\bar{\omega} + \bar{\omega}_c)(\bar{\lambda} - \bar{\omega}) - \bar{\omega}_c](\bar{\lambda}^2 - \bar{q}^2) + \bar{\alpha}(\bar{\lambda} - \frac{1}{4}\bar{\omega}) = 0, \quad (26)$$

where  $\bar{\omega} = -\omega/N\Omega$  is the normalized Doppler-shifted frequency (normalized resonance frequency),  $\bar{q} = (\hbar/2m)(k_r - k_s)^2/N\Omega$  is the normalized quantum parameter,  $\bar{\omega}_c = \omega_c/N\Omega$  denotes the normalized cyclotron frequency and  $\bar{\alpha} = [A_s(k_r - k_s)e/mN\Omega]^2$ .

In the above dispersion relation we have considered symmetrizing the momentum bunching and taken into account the term  $\sum_j \exp(-i\theta_j)p_j^2$ . Besides, we considered the resonance condition in the quantum regime  $\bar{\omega} = \bar{q}$ , so that  $\bar{\omega}/4 = \bar{k}$ , where  $\bar{k} = \hbar k^2/2mN\Omega$ .

In the quantum regime ( $\bar{\rho} < 1$ ), the momentum spread cannot be smaller than the photon recoil  $\hbar k$  and only a single frequency, corresponding to a single momentum transition, occurs with line width (Bonifacio *et al.*, 2007)

$$\left(\frac{\Delta\omega}{\omega}\right)_{\text{QFEL}} \simeq \frac{\lambda}{L_b}$$

where  $L_b$  denotes the electron bunch length. This equation means that a QFEL operating in the angstrom region with electron beam duration  $\tau = 1$  ps can generate radiation with a line width of  $10^{-7}$ , much smaller than the envelope line width of the classical spectrum (typically of the order of  $10^{-3}$ ). Therefore, the QFEL can be a very promising X-ray source, and a formidable tool for ultra-high-resolution process studies.

In the absence of the axial-guide magnetic field,  $\bar{\omega}_c = 0$ , and for a helical wiggler our dispersion relation (26) coincides with that of Bonifacio *et al.* (2006).

#### 4. Numerical studies and conclusion

A numerical study of the dispersion relation [equation (26)] is made in this section. The graph of the imaginary part of the complex root of equation (26) versus the normalized Doppler shifted frequency  $\bar{\omega}$  is shown in Fig. 1. As seen in this figure, when  $\bar{\omega}_c = 0$  (Fig. 1a), for  $\bar{q} = 0$  we have the classical result of a FEL without any initial energy spread. By going into the quantum regime, for  $\bar{q} = 0.5, 4, 7$  and  $10$  there is a special behavior in which the resonance occurs at  $\bar{\omega} = \bar{q}$ , with full width equal to  $2(2/\bar{q})^{1/2}$  and peak value  $\text{Im } \bar{\lambda} = (1/2\bar{q})^{1/2}$ . Here,  $\bar{q}$  represents the intrinsic quantum momentum spread. As a consequence,  $\text{Im } \bar{\lambda}$  decreases with increasing  $\bar{q}$ , so that the field and the bunching grow exponentially as  $\exp(-\text{Im } \bar{\lambda})t$ .

By turning the axial-guide magnetic field on so that  $\bar{\omega}_c \neq 0$  (Fig. 1b), in the quantum regime, we observed a decrease in the width and peak value for each chosen  $\bar{q}$ . As a consequence,  $\text{Im } \bar{\lambda}$  decreases with increasing  $\bar{\omega}_c$  (Fig. 1c), so that we will have an increase in the field and the bunching exponentially for a fixed value of  $\bar{q}$ . Also we observed a resonance shift in the presence of the external magnetic field, as shown in the figure.

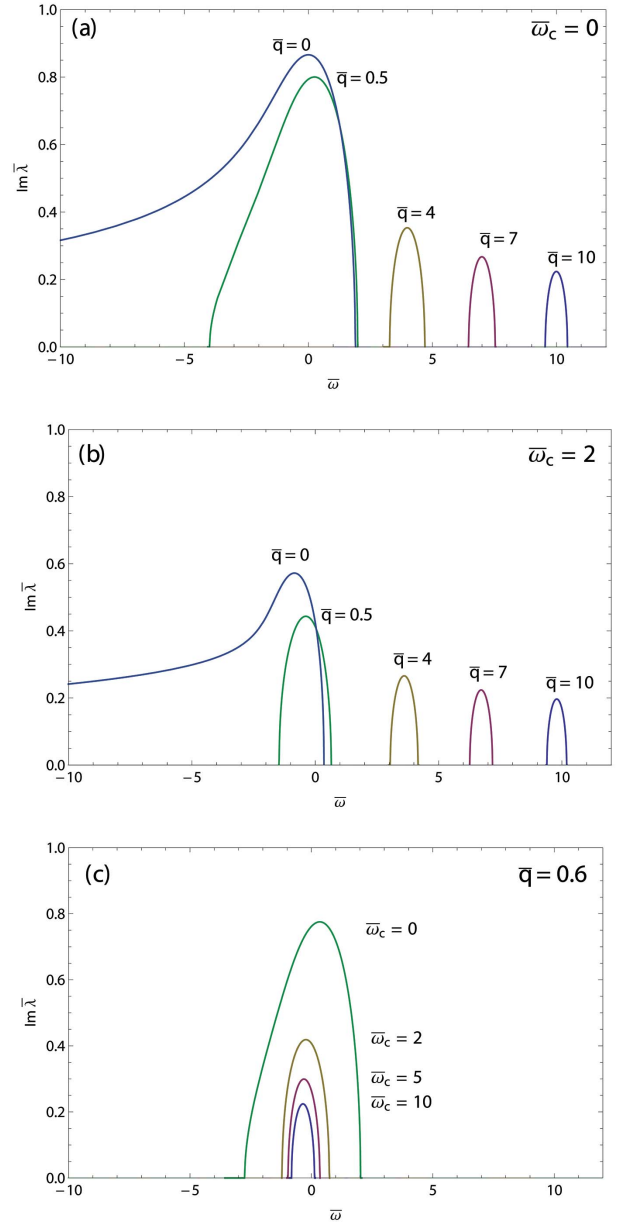


**Figure 1** Imaginary part of the complex root of the characteristic equation (26) versus  $\bar{\omega}$  for  $\bar{q} = 0, 0.5, 4, 7, 10$  with  $\bar{\omega}_c = 0$  (a) and  $\bar{\omega}_c = 2$  (b), and for  $\bar{q} = 0.6$  with  $\bar{\omega}_c = 0, 2, 5$  and  $10$  (c).

From Bonifacio *et al.* (2006), substituting  $\bar{\omega}$  for  $\Delta_n = 2n\bar{q} - \bar{\omega}_{\text{sh}}$  in equation (26) and plotting the imaginary part of  $\bar{\lambda}$  as a function of  $\bar{\omega}_{\text{sh}}$ , we obtain new graphs as shown in Fig. 2. In these figures,  $\bar{\omega}_{\text{sh}}$  is the normalized frequency shift proportional to  $(\bar{\omega}' - \bar{\omega})/\bar{\omega}$ , which describes the relative deviation of the radiation frequency from the normalized resonant frequency  $\bar{\omega}$ , and  $n$  refers to a momentum eigenvalue related to an arbitrary momentum eigenstate, which is initially occupied by the electrons.

When  $\bar{\omega}_c = 0$ , for  $\bar{q} = 5$ , as shown in Fig. 2(a<sub>1</sub>), it can be seen that the regions of the spectrum corresponding to gain ( $\text{Im } \bar{\lambda} > 0$ ) appear as a series of discrete lines corresponding to different values of  $n$ . Each of these lines is centered on

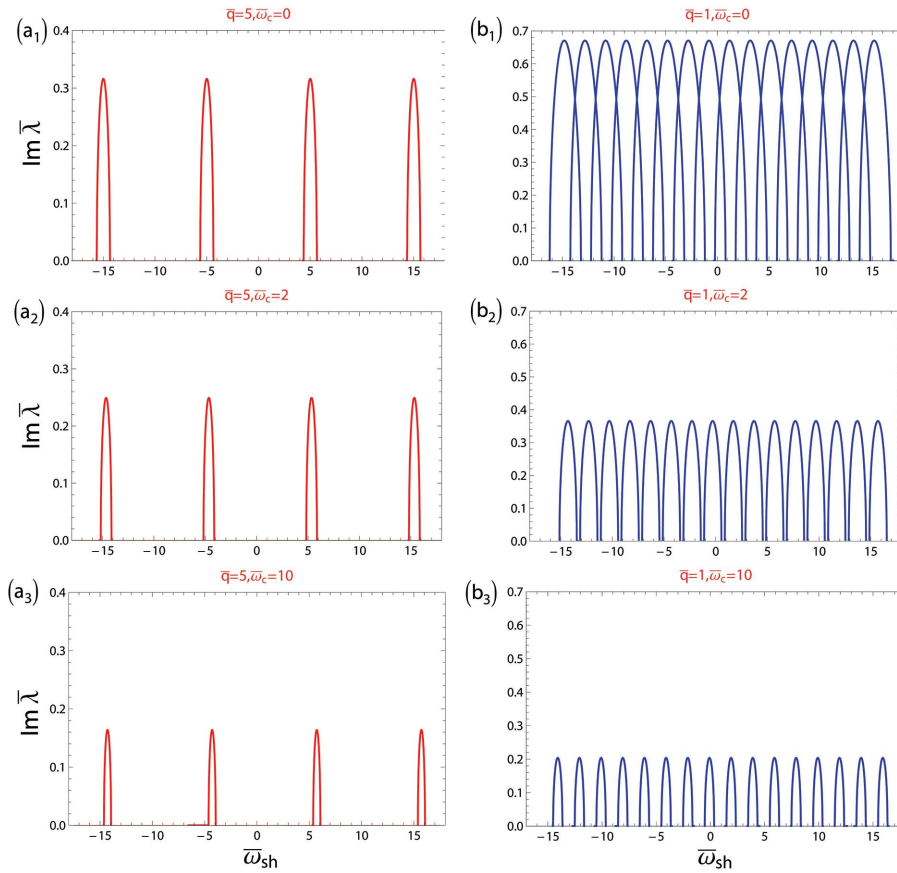


**Figure 2** Imaginary part of the unstable root of the characteristic equation (26) (with respect to transformation  $\bar{\omega} \rightarrow \Delta_n = 2n\bar{q} - \bar{\omega}_{sh}$ ) versus  $\bar{\omega}_{sh}$ , for  $\bar{q} = 1$  and  $\bar{\omega}_c$  equal to 0 ( $b_1$ ), 2 ( $b_2$ ) and 10 ( $b_3$ ), for  $\bar{q} = 5$  and  $\bar{\omega}_c$  equal to 0 ( $a_1$ ), 2 ( $a_2$ ) and 10 ( $a_3$ ).

$\bar{\omega}_{sh} = (2n - 1)\bar{q}$ , equally separated by a distance  $2\bar{q}$ , and has a width of  $2(2\bar{q})^{1/2}$ . As seen in Fig. 2( $b_1$ ), with a decrease in  $\bar{q}$ , in a certain span of  $\bar{\omega}_{sh}$  the number of lines increases and the discrete lines overlap with each other so that the spectrum turns into a classical one.

By turning the axial-guide magnetic field on ( $\bar{\omega}_c \neq 0$ ), we have observed a narrowing in spectrum lines for a fixed value of  $\bar{q}$ , Figs. 2( $b_2, b_3$ ) and 2( $a_2, a_3$ ), respectively, for  $\bar{q} = 1$  and  $\bar{q} = 5$  [Figs. 2( $a_2, b_2$ ) and 2( $a_3, b_3$ ) correspond to  $\bar{\omega}_c = 2$  and 10, respectively]. As seen in Fig. 2, with an increase in  $\bar{\omega}_c$ , for a

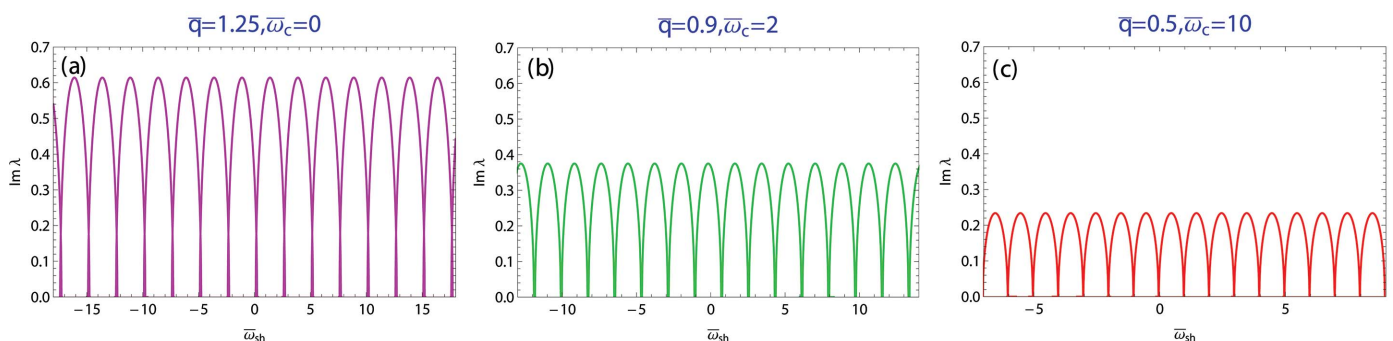


**Figure 3** Imaginary part of the unstable root of the characteristic equation (26) versus  $\bar{\omega}_{sh}$ . The spectrum lines overlap each other when  $\bar{\omega}_c = 0$  (a) for  $\bar{q} < 1.25$ ,  $\bar{\omega}_c = 2$  (b) for  $\bar{q} < 0.9$  and  $\bar{\omega}_c = 10$  (c) for  $\bar{q} < 0.5$ .

fixed value of  $\bar{q}$ , the width and peak value ( $\text{Im } \bar{\lambda}$ ) of the spectrum lines decreases and the distance separation of the lines remains constant as  $2\bar{q}$ . In Fig. 3,  $\text{Im } \bar{\lambda}$  versus  $\bar{\omega}_{sh}$  has been plotted for the various spectrum lines overlapping conditions. As shown in Fig. 3, the upper limit for  $\bar{q}$  to overlap the spectrum lines decreases with increasing  $\bar{\omega}_c$ , so that for  $\bar{\omega}_c = 0$  (a) overlapping takes place for  $\bar{q} < 1.25$ , while for  $\bar{\omega}_c = 2$  (b) overlapping occurs for  $\bar{q} < 0.9$ , and for  $\bar{\omega}_c = 10$  (c) we have  $\bar{q} < 0.5$ .

The fundamental feature of the quantum FEL with plasma-wave pumping in the presence of an axial magnetic field is an extremely narrow single-line radiation spectrum, whose line width can be some orders of magnitude smaller than the bandwidth of conventional quantum FELs (see Fig. 2).

As an example, we consider a QFEL producing radiation at a wavelength of 6 nm in the quantum regime using a plasma whistler wiggler with a wavelength of 32  $\mu\text{m}$  and effective wiggler parameter  $K = 0.1$ . The electron beam energy can be approximately 36 MeV, and the axial magnetic field strength is  $B_0 = 0.7$  kG (for  $\bar{\omega}_c = 2$ ) for a plasma density  $n_p = 0.86 \times 10^{18} \text{ cm}^{-3}$ .

In summary, in this paper we have studied the role of the axial-guide magnetic field on plasma-whistler-pumped free-electron laser operation, which operates in the quantum regime. Employing a plasma wave as a wiggler is attractive for two reasons. First, the effective wiggler strength can be extremely large and, second, the effective wavelength is shorter than that available with a conventional magnetic wiggler. Using plasma densities in the  $10^{18} \text{ cm}^{-3}$  range, a wiggler wavelength of the order of 30  $\mu\text{m}$  can be obtained, thereby permitting production of very short wavelength

radiation ( $\sim \text{\AA}$ ) with modest energy beams. We began from the derivation of an  $N$ -particle three-dimensional Hamiltonian in a quantum approach in which the vertical motion of electrons was controlled by a transverse operator, and then, by using the Heisenberg evolution equation, the dynamics of the system in the linear regime was determined. With respect to the transverse operator, a new functional collective operator was introduced and the characteristic equation as a dispersion relation was then obtained, for a fixed value of the normalized quantum parameter ( $\bar{q}$ ), showing a shift and narrowing of the FEL resonance and decrease in peak value, which caused a growth in the field and bunching exponentially. In addition, we observed the quantum SASE affected by the normalized cyclotron frequency ( $\bar{\omega}_c$ ), so that, for a fixed value of  $\bar{q}$ , by increasing  $\bar{\omega}_c$  the spectrum becomes a series of discrete narrow lines and we obtained an upper limit for  $\bar{q}$ , which depends on the value of  $\bar{\omega}_c$ ; for values of  $\bar{q}$  smaller than this limit the spectrum lines overlap each other. A plasma-based FEL operating in the quantum regime can provide a compact and monochromatic X-ray source, which is a formidable tool for ultra-high-resolution process studies.

## References

- Abbasi, E., Jafari, S. & Hedayati, R. (2016). *J. Synchrotron Rad.* **23**, 1282–1295.
- Allaria, E., Callegari, C., Cocco, D., Fawley, W. M., Kiskinova, M., Masciovecchio, C. & Parmigiani, F. (2010). *New J. Phys.* **12**, 075002.
- Altarelli, M. (2006). Editor. *The European X-ray FEL Technical Design Report*, DESY Report 2006–097. DESY, Hamburg, Germany.
- Andriyash, I. A., Tikhonchuk, V. T., Malka, V., D’Humières, E. & Balcou, Ph. (2015). *Phys. Rev. ST Accel. Beams*, **18**, 050704.
- Arthur, J. (2002). Conceptual Design Report No. SLAC-R-593. Stanford Synchrotron Radiation Laboratory, Stanford, CA, USA.
- Avetissian, H. K. & Mkrtchian, G. F. (2007). *Phys. Rev. ST Accel. Beams*, **10**, 030703.
- Bambini, A. & Renieri, A. (1978). *Lett. Nuov. Cim.* **21**, 399.
- Bonifacio, R., Cola, M. M., Piovella, N. & Robb, G. R. M. (2005a). *Europhys. Lett.* **69**, 55–60.
- Bonifacio, R., Fares, H., Ferrario, M., McNeil, B. W. J. & Robb, G. R. M. (2017). *Opt. Commun.* **382**, 58–63.
- Bonifacio, R., Piovella, N., Cola, M. M. & Volpe, L. (2007). *Nucl. Instrum. Methods Phys. Res. A*, **577**, 745–750.
- Bonifacio, R., Piovella, N., Cola, M. M., Volpe, L., Schiavi, A. & Robb, G. R. M. (2008). *Nucl. Instrum. Methods Phys. Res. A*, **593**, 69–74.
- Bonifacio, R., Piovella, N. & Robb, G. R. M. (2005b). *Nucl. Instrum. Methods Phys. Res. A*, **543**, 645–652.
- Bonifacio, R., Piovella, N., Robb, G. R. M. & Schiavi, A. (2006). *Phys. Rev. ST Accel. Beams*, **9**, 090701.
- Freund, H. P. & Antonsen, J. M. (1996). *Principles of Free-Electron Lasers*. London: Chapman & Hall.
- Ganeev, R. A. (2012). *Laser Phys. Lett.* **9**, 175–194.
- Geloni, G., Kocharyan, V. & Saldin, E. (2010). *Scheme for Generation of Highly Monochromatic X-rays From a Baseline XFEL Undulator*, DESY Report 10–033. DESY, Hamburg, Germany.
- Hedayati, R., Jafari, S. & Batebi, S. (2017). *High. Energy Density Phys.* **23**, 138–152.
- Jafari, S. (2015). *Laser Phys. Lett.* **12**, 075002.
- Jafarinia, F., Jafari, S. & Mehdian, H. (2013). *Phys. Plasmas*, **20**, 043106.
- Joshi, C., Katsouleas, T., Dawson, J. M., Yan, Y. T. & Slater, J. M. (1987). *IEEE J. Quantum Electron.* **23**, 1571–1577.
- Kiselev, S., Pukhov, A. & Kostyukov, I. (2004). *Phys. Rev. Lett.* **93**, 135004.
- Mandl, F. & Shaw, G. (2010). *Quantum Field Theory*, 2nd ed. New York: John Wiley and Sons, Ltd.
- McNeil, B. W. J. & Thompson, N. R. (2010). *Nat. Photon.* **4**, 814.
- Ratner, D., Abela, R., Amann, J., Behrens, C., Bohler, D., Bouchard, G., Bostedt, C., Boyes, M., Chow, K., Cocco, D., Decker, F. J., Ding, Y., Eckman, C., Emma, P., Fairley, D., Feng, Y., Field, C., Flechsig, U., Gassner, G., Hastings, J., Heimann, P., Huang, Z., Kelez, N., Krzywinski, J., Loos, H., Lutman, A., Marinelli, A., Marcus, G., Maxwell, T., Montanez, P., Moeller, S., Morton, D., Nuhn, H. D., Rodes, N., Schlotter, W., Serkez, S., Stevens, T., Turner, J., Walz, D., Welch, J. & Wu, J. (2015). *Phys. Rev. Lett.* **114**, 054801.
- Robb, G. R. & Bonifacio, R. (2012). *Phys. Plasmas*, **19**, 073101.
- San-kui, G. (1992). *Phys. Rev. A*, **46**, 1140–1143.
- Schroeder, C. B., Pellegrini, C. & Chen, P. (2001). *Phys. Rev. E*, **64**, 056502.
- Sen Gupta, D. N. (1991). *Phys. Lett. A*, **152**, 453–457.
- Sharma, A. & Tripathi, V. K. (1996). *Phys. Plasmas*, **3**, 3116–3120.
- Stenholm, S. & Bambini, A. (1981). *IEEE J. Quantum Electron.* **17**, 1363–1371.
- Tanaka, T. & Shintake, T. (2005). Editors. *SCSS X-FEL 2005 Conceptual Design Report*. Japan: RIKEN.